

SIDEBANDS DUE TO QUASI-PERIODIC OSCILLATIONS IN 4U 1626–67

Jefferson M. Kommers, Deepto Chakrabarty, & Walter H. G. Lewin

*Department of Physics and Center for Space Research,
Massachusetts Institute of Technology, Cambridge, MA 02139*

To appear in ApJ Letters

Contact: kommers@space.mit.edu

ABSTRACT

The low-mass X-ray binary pulsar 4U 1626–67 shows 0.048 Hz quasi-periodic oscillations (QPOs) and red noise variability as well as coherent pulsations at the 0.130 Hz neutron star spin frequency. Power density spectra of observations made with the *Rossi X-ray Timing Explorer* show significant sidebands separated from the pulsar spin frequency (and its harmonics) by the QPO frequency. These show that the instantaneous amplitude of the coherent pulsations is modulated by the amplitude of the QPOs. This phenomenon is expected in models such as the magnetospheric beat frequency model where the QPOs originate near the polar caps of the neutron star. In the 4–8 keV energy range, however, the lower-frequency sidebands are significantly stronger than their higher-frequency complements; this is inconsistent with the magnetospheric beat frequency model. We suggest that the 0.048 Hz QPOs are instead produced by a structure orbiting the neutron star at the QPO frequency. This structure crosses the line of sight once per orbit and attenuates the pulsar beam, producing the symmetric (amplitude modulation) sidebands. It also reprocesses the pulsar beam at the beat frequencies between the neutron star spin frequency and the QPOs, producing the excess variability observed in the lower-frequency sidebands. Quite independently, we find no evidence that the red noise variability modulates the amplitude of the coherent pulsations. This is also in contrast to the expectations of the magnetospheric beat frequency model and differs from the behavior in some high-mass X-ray binary pulsars.

Subject headings: X-rays: general — stars: neutron

1. Introduction

Quasi-periodic oscillations (QPOs) have been detected in at least 9 accretion-powered binary X-ray pulsars (see Takeshima et al. 1994 and references therein; also Finger, Wilson, & Harmon 1996; Belloni & Hasinger 1990; Zhang et al. 1996; Kommers et al. 1997). Several physical mechanisms have been proposed to explain the QPOs in X-ray binaries (see Lewin, van Paradijs, & van der Klis 1988; van der Klis 1995 for reviews). One well-developed model is the magnetospheric beat frequency model (MBFM) in which the QPO centroid frequency (ν_{QPO}^{MBFM}) represents the beat frequency between the Keplerian orbital frequency at the inner edge of the accretion disk (ν_K) and the neutron star spin frequency (ν_s): $\nu_{QPO}^{MBFM} = \nu_K - \nu_s$ (Alpar & Shaham 1985; Lamb et al. 1985). Another model, which has received less discussion in the literature, is the Keplerian frequency model (KFM; Bath, Evans, & Papaloizou 1974; van der Klis et al. 1987). In the KFM, inhomogeneities in the plasma orbiting at the inner edge of the accretion disk modulate the X-ray intensity by varying the optical depth along the line of sight; the QPO frequency equals the Keplerian frequency at the inner edge of the disk ($\nu_{QPO}^{KFM} = \nu_K$).

4U 1626–67 is a low-mass X-ray binary (LMXB) pulsar with a 7.67 s pulse period (130 mHz spin frequency). Despite extensive searches, no Doppler shifts have been detected in the X-ray pulse arrival times (Levine et al. 1988; Shinoda et al. 1990; Chakrabarty et al. 1998). The presence of a low-mass companion star in a 42 minute prograde orbit around the neutron star is inferred from photometric timing measurements on the optical counterpart, KZ TrA, which shows pulsations at the same frequency as the X-ray pulsations. The power spectrum of the optical variability shows additional weak pulsations in a sideband 0.4 mHz below the main optical pulsation frequency (Middleditch et al. 1981; Chakrabarty 1998). The interpretation is that the sideband represents X-rays from the pulsar beam that have been reprocessed on the surface of the companion star. The 0.4 mHz shift to lower frequencies results from the lower apparent pulsar frequency observed in a frame rotating with the binary orbit of the companion (Middleditch et al. 1981).

The long-term behavior of the X-ray pulse frequency has been discussed by Chakrabarty et al. (1997). Although the pulsar was spinning up ($\dot{\nu}_s > 0$)

for more than 13 years after its discovery, it experienced a torque reversal in approximately June 1990. It has been spinning down ($\dot{\nu}_s < 0$) ever since (Chakrabarty et al. 1997).

QPOs at 48 mHz with fractional root-mean-square (rms) amplitudes as high as 17% have been seen in X-ray observations with *Ginga* (Shinoda et al. 1990), *ASCA* (Angelini et al. 1995), and *RXTE* (Chakrabarty 1998). Chakrabarty (1998) recently detected these QPOs in the optical *U*, *B*, and *R* bands.

In this *Letter* we present evidence that neither the MBFM nor the KFM provides a suitable explanation for the 48 mHz QPOs in 4U 1626–67. We propose instead that the QPOs are produced by some kind of coherent structure (a “blob”) orbiting the neutron star with an orbital frequency equal to the QPO frequency, but the “blob” is not at the inner edge of the accretion disk.

2. Observations and Analysis

4U 1626–67 was observed with the *Rossi X-ray Timing Explorer* for a total of 150 ks on 1996 February 10–15¹. The photon arrival times from the Proportional Counter Array (PCA) were transformed to the solar system barycenter frame and binned at 0.125 s. Two energy ranges were selected, 4–8 keV and 17–30 keV. For each energy range, the observations were partitioned into 400 s intervals. Any intervals that contained data gaps or spacecraft slews were omitted from further analysis. The data for each of the 340 surviving intervals were flattened by subtracting the best-fit cubic polynomial and then Fourier transformed to obtain a power spectrum. An ensemble-averaged power spectrum for each energy range was obtained by averaging the individual power spectra. Uncertainties in the average powers were computed from the sample variance of the individual powers at each Fourier frequency. These average power spectra are shown in Figure 1.

Several power spectral components can be identified in Figure 1. The feature at 48 mHz represents the QPOs identified previously (see section 1). The set of sharp peaks at integer multiples of 130 mHz represents the harmonic structure of the coherent pulsations (CPs). A further red-noise (RN) component is apparent up to ~ 1 Hz. A local maximum in the

¹These observations will be discussed further by Chakrabarty et al. (1998).

RN component appears around 10 mHz, but this may be an artifact of the detrending procedure that was applied before taking the Fourier transforms.

The finite length (400 s) of the Fourier transforms creates troublesome side lobes around the CP peaks in the power spectrum (see Figure 1). To suppress these and other complications related to the presence of the coherent pulsations in the data, we constructed a pulse-subtracted power spectrum. For each 400 s data segment, a fiducial pulse profile was obtained by folding the count rates according to the frequency model given by Chakrabarty et al. (1997). This pulse profile was subtracted from the data before taking the Fourier transforms and constructing the average pulse-subtracted power spectra.

For both energy ranges a best-fit model for the obvious RN, QPO, and constant components of the pulse-subtracted power spectrum was found by χ^2 minimization. A sum of two Lorentzian profiles was used for the RN component and a single Lorentzian was used for the QPO component. The contributions of each component to the total best-fit models are shown as dotted curves in Figure 1. Although this functional form provided a reasonable representation of the gross features of the power spectra, the fits were formally unacceptable. The reduced chi-squared values were $\chi^2_\nu = 1.41$ in the 4–8 keV range and $\chi^2_\nu = 1.29$ in the 17–30 keV range for 1526 degrees of freedom. The data therefore support consideration of more detailed models.

In the 4–8 keV range the best-fit model parameters for the QPO component yield a fractional rms variability (R), corrected for background, of $14.4 \pm 0.4\%$, a centroid frequency (ν_0) of 48.5 ± 0.2 mHz, and a FWHM (Γ) of 8.5 ± 0.5 mHz. In the 17–30 keV range the QPO parameters are $R = 22.4 \pm 0.5\%$, $\nu_0 = 48.2 \pm 0.2$ mHz, and $\Gamma = 9.3 \pm 0.6$ mHz.

To look for more subtle features in the power spectra, we produced residuals by subtracting the best-fit model from each pulse-subtracted power spectrum. Portions of these residuals below 600 mHz are shown in Figure 2. The arrows in Figure 2 show the positions where sidebands are expected if the QPO signal modulates the amplitude of the coherent pulsations. The origin of these sidebands is the Fourier frequency-shifting theorem: if a sinusoidal signal, $\cos(2\pi\nu_s t)$, has a time-varying amplitude, $f(t)$, then the Fourier transform of the source intensity contains terms proportional to $F(\nu \pm \nu_s)$, where $F(\nu)$ is the Fourier transform of $f(t)$ (for a complete discussion in the

context of the red-noise variability in X-ray pulsars see Lazzati & Stella 1997; Burderi et al. 1997). If $f(t)$ represents the QPO signal then its power spectrum $|F(\nu)|^2$ has a local maximum at the QPO centroid frequency. If $f(t)$ also modulates the instantaneous amplitude of the coherent pulsations, the terms in the power spectrum proportional to $|F(n\nu_s \pm \nu_{QPO})|^2$ produce symmetric sidebands in the shape of the QPO peak around the frequencies $n\nu_s$, where $n = 1, 2, \dots$ is an integer. Panel (a) of Figure 2 shows evidence for this effect, especially around the second (390 mHz) and third (520 mHz) harmonics of the spin frequency. Panel (b) shows strong symmetric sidebands around the fundamental (130 mHz).

A phenomenon that emits X-rays at the beat frequencies between the pulsar harmonics and another oscillation (such as the QPOs) will produce sidebands that appear either on the lower-frequency sides or on the higher-frequency sides (but not both) of the harmonic frequencies. Panel (a) of Figure 2 shows a clear example of this. The sidebands on the lower-frequency sides of the fundamental (130 mHz) and the first harmonic (260 mHz) are much stronger than the complementary sidebands on the higher-frequency sides. Additional oscillations in the source intensity must be present at these beat frequencies (82 mHz and 212 mHz).

For greater sensitivity to the sidebands seen in Figure 2, we produced harmonically folded residuals. The residuals from the neighborhood of each harmonic were shifted down to the fundamental and summed. Figure 3 shows the folded residuals. The dotted lines show the position of the pulsar frequency.

We fitted independent Lorentzian profiles to each of the sidebands in the folded residuals to measure the total rms variability contained in them. For the lower-frequency sideband in the 4–8 keV range, we found $R = 5.7 \pm 0.4\%$, $\nu_0 = 83.2 \pm 0.6$ mHz, and $\Gamma = 8.8 \pm 0.2$ mHz; for the higher-frequency sideband, we found $R = 2.4 \pm 0.4\%$, $\nu_0 = 176.6 \pm 0.8$ mHz, and $\Gamma = 4.3 \pm 0.3$ mHz. For the lower-frequency sideband in the 17–30 keV range, we found $R = 8.3 \pm 0.5\%$, $\nu_0 = 83.2 \pm 0.7$ mHz, and $\Gamma = 6.2 \pm 1.3$ mHz; for the higher-frequency sideband, we found $R = 7.5 \pm 0.5\%$, $\nu_0 = 177.6 \pm 0.6$ mHz, and $\Gamma = 5.5 \pm 1.2$ mHz.

We note that the folded residuals show no obvious sidebands in the shape of the RN power spectrum components, consistent with an *absence* of amplitude modulation of the pulse intensity by the RN variability. In the 4–8 keV and 17–30 keV ranges, our fits to

the folded residuals place 90%-confidence upper limits of 2.3% and 3.1% (respectively) on the total rms variability contained in symmetric sidebands due to amplitude modulation of the coherent pulses by the RN variability. These upper limits depend on the functional form used to model the RN components, however.

3. Discussion

Significant sidebands are detected around the 130 mHz pulsar frequency and its harmonics in power density spectra of 4U 1626–67. The sidebands appear at frequencies $n\nu_s \pm \nu_{QPO}$, where $n = 1, 2, \dots$ is an integer. In the 17–30 keV range the sidebands are mirror images of each other: they are symmetric in both frequency and power amplitude. We will refer to these as “symmetric” side bands. In the 4–8 keV range, however, the lower-frequency sidebands contain significantly more power than the higher-frequency ones: they are symmetric in frequency but *not* in power amplitude. We will assume that these “asymmetric” sidebands represent the superposition of underlying symmetric sidebands *plus* some additional power at the lower sideband frequencies ($n\nu_s - \nu_{QPO}$). We will refer to this excess power as “enhanced lower-frequency” sidebands.

The presence of the symmetric sidebands suggests that the instantaneous amplitude of the coherent pulsations contains a term proportional to the 48 mHz QPO signal. This phenomenon is expected in models where some of the QPOs are produced near the polar caps of the neutron star. In the magnetospheric beat frequency model (MBFM), for example, magnetically gated clumps of matter from the inner accretion disk would follow the magnetic field lines onto the polar caps and modulate the X-ray intensity there (Alpar & Shaham 1985; Lamb et al. 1985). Symmetric sidebands could also occur in models such as the Keplerian frequency model (KFM) where inhomogeneities in the accretion disk quasi-periodically absorb some of the pulsar beam along the line of sight.

The presence of the enhanced lower-frequency sidebands shows that the situation is more complicated, however. In the 4–8 keV range at least two of the lower-frequency sidebands (the one at $\nu_s - \nu_{QPO} = 82$ mHz and the one at $2\nu_s - \nu_{QPO} = 212$ mHz) are much stronger than their higher-frequency complements. Since amplitude modulation produces symmetric sidebands, there must be a physical mechanism

that produces additional variability at the frequencies $n\nu_s - \nu_{QPO}$. Neither the MBFM nor the KFM (as usually formulated) provides a satisfactory explanation for both the main QPO signal and the enhanced lower-frequency sidebands.

In the MBFM the QPOs represent a beat frequency between the Keplerian frequency at the magnetopause and the pulsar frequency ($\nu_{QPO}^{MBFM} = \nu_K - \nu_s$). If we set $\nu_K = 178$ mHz, the MBFM would predict the 48 mHz QPOs. The presence of symmetric sidebands would follow since the 48 mHz oscillations occur in the accretion stream near the neutron star’s polar caps. But this MBFM provides no mechanism that allows the QPOs to again “beat” against the rotating pulsar beam to produce the enhanced lower-frequency sidebands at $\nu_s - \nu_{QPO} = 82$ mHz and $2\nu_s - \nu_{QPO} = 212$ mHz (Alpar & Shaham 1985; Lamb et al. 1985; Shibazaki & Lamb 1987).

The KFM can explain the sideband structure (see our modified version of this model below) but not the direct QPOs. This is because the KFM cannot explain QPOs with centroid frequencies *less* than the neutron star spin frequency. In the KFM the QPO frequency would be the Keplerian frequency at the inner edge of the accretion disk (Bath et al. 1974; van der Klis et al. 1987). Since the QPO centroid frequency is less than the pulsar spin frequency in 4U 1626–67, the inner edge of the disk would lie outside the co-rotation radius. Centrifugal forces exerted by the rotating neutron star magnetosphere would therefore inhibit accretion (the “propeller effect”; Illarionov & Sunyaev 1975). The radius corresponding to a 48 mHz Keplerian orbital frequency is $r_K = 1.3 \times 10^9$ cm, which exceeds the co-rotation radius $r_{co} = 6.5 \times 10^8$ cm. The location of the inner edge of the disk is less certain: depending on the distance to the source, r_K could exceed the Alfvén radius, $r_A \approx 3 \times 10^9 d_{\text{kpc}}^{-4/7}$ cm $\approx 9 \times 10^8$ cm, where we have assumed a distance of 8 kpc and used the measurements by Orlandini et al. (1997) of the 0.1–100 keV luminosity ($L_X = 6.6 \times 10^{34}$ erg s⁻¹ d_{kpc}^2) and magnetic field strength ($B = 3.3 \times 10^{12}$ G).

If we dispense with the KFM’s requirement that the QPO frequency represents the *Keplerian frequency at the inner edge of the disk*, however, we obtain a scenario that can simultaneously account for the direct QPOs, the symmetric sidebands, and the enhanced lower-frequency sidebands. Suppose a large coherent structure (a “blob”) of material orbits the

neutron star with a frequency roughly equal to the QPO centroid frequency (48 mHz); this may or may not represent the Keplerian frequency at the radius of the blob. We use the term “blob” to distinguish this structure from the “clumps” of the MBFM (Lamb et al. 1985) and the “inhomogeneities” of the KFM (Bath et al. 1974). The direct QPO signal is produced as the “blob” modulates the optical depth to the accretion disk as it orbits. Once every orbit a portion of the “blob” crosses the line of sight between the neutron star and the Earth and scatters X-rays from the pulsar beam out of the line of sight. This quasi-periodic attenuation of the pulsar beam intensity produces the symmetric sidebands around the spin frequency and its harmonics.

Suppose also that the “blob” orbits in the same sense as the pulsar rotation, so it is illuminated by the pulsar beam with a frequency of $\nu_s - \nu_{QPO} = 82$ mHz. The first harmonic illuminates the “blob” with a frequency of $2\nu_s - \nu_{QPO} = 212$ mHz. When the “blob” is not crossing the line of sight between the neutron star and the Earth, it reprocesses X-rays from the pulsar beam and returns some of them along the line of sight. The reprocessed radiation appears as oscillations at the frequencies of the enhanced lower-frequency sidebands, $n\nu_s - \nu_{QPO}$. The situation is analogous to the reprocessing of the pulsar beam by the companion star (Middleditch et al. 1981; Chakrabarty 1998). The overall scenario is similar to the production of orbital sidebands due to the modulation of pulsations in intermediate polars (Warner 1986).

The fact that the enhanced lower-frequency sidebands are found only below the fundamental (130 mHz) and the first harmonic (260 mHz) in the 4–8 keV range needs an explanation. We suggest that this is related to the reprocessing of the pulsar beam. In the 17–30 keV range the pulse profile is dominated by the fundamental and the first harmonic (see Figure 1). If the “blob” reprocesses hard X-rays and emits them at lower energies, the strengths of the sidebands at 82 mHz and 212 mHz in the 4–8 keV range would reflect the strengths of the corresponding pulse profile harmonics at *higher* energies (e.g. 17–30 keV).

The nature of the reprocessing “blob” is not clear. It is unlikely that there are many “blobs” scattered around the 48 mHz orbit, because reprocessed emission from these would contribute with many different phases and tend to wash out the oscillations responsible for the enhanced lower-frequency sidebands. On the other hand, it is not clear why a single reprocess-

ing structure of limited spatial extent would survive in the accretion disk against the differential rotation of nearby Keplerian orbits. The QPOs appear to be stable on the time scale of a decade or more, having been first observed in 1988 (Shinoda et al. 1990).

It is perhaps more likely that the orbital frequency of the “blob” is *not* Keplerian. For example, the “blob” may represent a superposition of oscillatory modes traveling as a stable wave packet around the accretion disk. Alpar & Yilmaz (1997) have described models of the normal-branch and horizontal-branch QPOs in LMXBs in terms of wave packets of sound waves in the accretion disk.

To our knowledge the sideband structure has not been previously used as a diagnostic of the QPO mechanism in X-ray pulsars. Regardless of whether the simple model we set forth above can stand up to closer scrutiny, the sideband structure provides remarkably constraining information on the possible QPO mechanisms. An unusual sideband structure was recently detected in the high-mass X-ray binary (HMXB) pulsar Cen X-3 (M. Finger, private communication, 1997) that may require a different interpretation than the one discussed here.

On the other hand, the sideband structure has been used to consider the origin of RN variability in X-ray pulsars (Burderi et al. 1997; Lazzati & Stella 1997). If the RN is produced by inhomogeneities in the accretion flow onto the magnetic poles of the neutron star, then the instantaneous amplitude of the coherent pulsations should contain a term proportional to the RN signal (just as for the QPO signal discussed above). For example, in the MBFM the same magnetically gated clumps that produce the QPOs are expected to create a RN component that represents the frequency content and lifetime broadening of the shots produced by each clump (Lamb et al. 1985; Shibazaki & Lamb 1987). The MBFM does not rule out the possibility of additional sources of RN variability that are unrelated to the magnetic gating mechanism, however.

We found no detectable modulation of the pulsar beam by the RN component in 4U 1626–67 (see Figure 1) even though the QPO signal modulates the pulsar beam substantially. The fractional rms variability between 0.0025 Hz and ~ 1 Hz in the combined 4–8 keV RN components was $42.5 \pm 0.5\%$; and that in the combined 17–30 keV RN components was $63.2 \pm 0.6\%$. Yet the upper limits on the total rms contained in the sidebands that would result from a modulation of the coherent pulses by the RN are only $\sim 3\%$. This sug-

gests that most of RN does *not* originate near the polar caps. This is in contrast to case of the HMXB pulsars SMC X-1, Vela X-1, 4U 1145–62, and possibly Cen X-3, in which the RN variability does appear to modulate the coherent pulse amplitude (Burderi et al. 1997; Lazzati & Stella 1997).

To summarize, we have detected sidebands around the neutron star spin frequency and its harmonics in 4U 1626–67. These show that the QPOs modulate the amplitude of the coherent pulsations. The presence of the enhanced lower-frequency sidebands below the pulsar frequency and its harmonics is inconsistent with the MBFM. Interpreting the lower-frequency sidebands as reprocessed radiation from the pulsar beam, we have proposed a modification of previous (Keplerian frequency) obscuration models that explains the observed QPOs and sideband structure. The strong RN component below 1 Hz does not appear to significantly modulate the amplitude of the coherent pulsations.

We thank Mark Finger and Brian Vaughan for useful discussions regarding the data analysis, and Dimitrios Psaltis and Michiel van der Klis for comments on the manuscript. J. M. K. acknowledges support from a NASA Graduate Student Researchers Program Fellowship NGT8-52816. D. C. was supported by a NASA *Compton GRO* Postdoctoral Fellowship under grant NAG5-3109. W. H. G. L. acknowledges support from NASA.

REFERENCES

- Alpar, M. A., & Shaham, J. 1985, *Nature*, 316, 239
- Alpar, M. A., & Yilmaz, A. 1997, *New Astronomy*, 2, 225
- Angelini, L., White, N. E., Nagase, F., Kallman, T. R., Yoshida, A., Takeshima, T., Becker, C., & Paerels, F. 1995, *ApJ*, 449, L41
- Bath, G. T., Evans, W. D., & Papaloizou, J. 1974, *MNRAS*, 167, 7P
- Belloni, T., & Hasinger, G. 1990, *A&A*, 230, 103
- Burderi, L., Robba, N. R., La Barbera, N., & Guainazzi, M. 1997, *ApJ*, 481, 943
- Chakrabarty, D. 1998, *ApJ*, 492, 342
- Chakrabarty, D., et al. 1997, *ApJ*, 474, 414
- Chakrabarty, D., et al. 1998, in preparation
- Finger, M. H., Wilson, R. B., & Harmon, B. A. 1996, *ApJ*, 459, 288
- Illarionov, A. F. & Sunyaev, R. A. 1975, *A&A*, 39, 185
- Kommers, J. M., Fox, D. W., Lewin, W. H. G., Rutledge, R. E., van Paradijs, J., & Kouveliotou, C. 1997, *ApJ*, 482, L53
- Lamb, F. K., Shibazaki, N., Alpar, M. A., & Shaham, J. 1985, *Nature*, 317, 681
- Lazzati, D., & Stella, L. 1997, *ApJ*, 476, 267
- Levine, A., Ma, C. P., McClintock, J., Rappaport, S., van der Klis, M., & Verbunt, F. 1988, *ApJ*, 327, 732
- Lewin, W. H. G., van Paradijs, J., & van der Klis, M. 1988, *Space Sci. Rev.*, 46, 273
- Middleditch, J., Mason, K. O., Nelson, J. E., & White, N. E. 1981, *ApJ*, 244, 1001
- Orlandini, M., et al. 1997, *astro-ph/9712023*
- Shibazaki, N., & Lamb, F. K. 1987, *ApJ*, 318, 767
- Shinoda, K., Kii, T., Mitsuda, K., Nagase, F., Tanaka, Y., Makishima, K., & Shibazaki, N. 1990, *PASJ*, 42, L27
- Takeshima, T., Dotani, T., Mitsuda, K., & Nagase, F. 1994, *ApJ*, 436, 871
- van der Klis, M. 1995, in *X-ray Binaries*, eds. W. H. G. Lewin, J. van Paradijs, & E. P. J. van den Heuvel (Cambridge University Press), 252
- van der Klis, M., Stella, L., White, N., Jansen, F., & Parmar, A. N. 1987, *ApJ*, 316, 411
- Warner, B., *MNRAS*, 219, 347
- Zhang, W., Morgan, E., Jahoda, K., Swank, J., Strohmayer, T., Jernigan, G., & Klein, R. 1996, *ApJ*, 469, L29

This 2-column preprint was prepared with the AAS L^AT_EX macros v4.0.

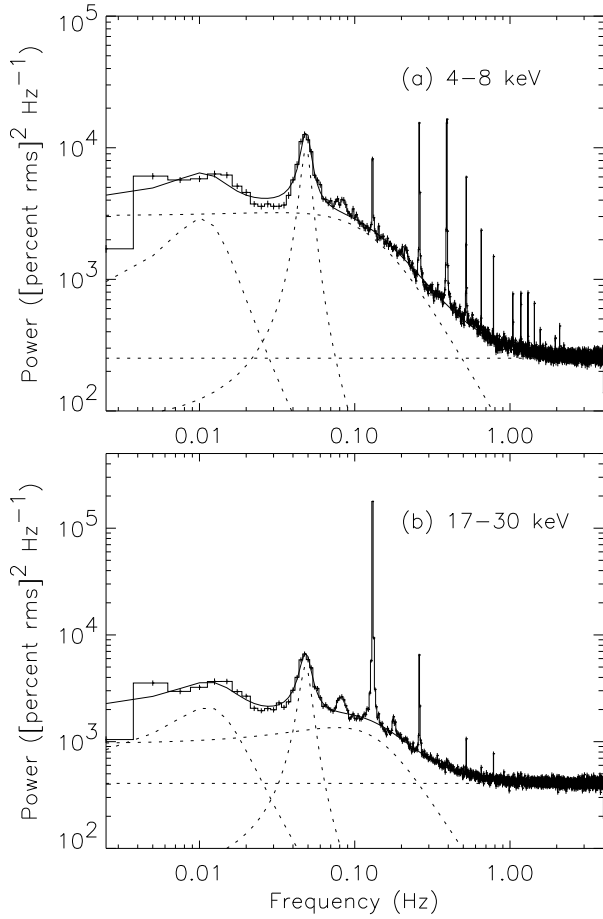


Fig. 1.— Ensemble averaged power spectra of 4U 1626–67 (histogram). The upper panel is from the 4–8 keV energy range, and the lower panel is from the 17–30 keV range. The best-fit models for the pulse-subtracted power spectrum components are also shown (solid line). The dotted lines show the contributions from each additive term in the best-fit models.

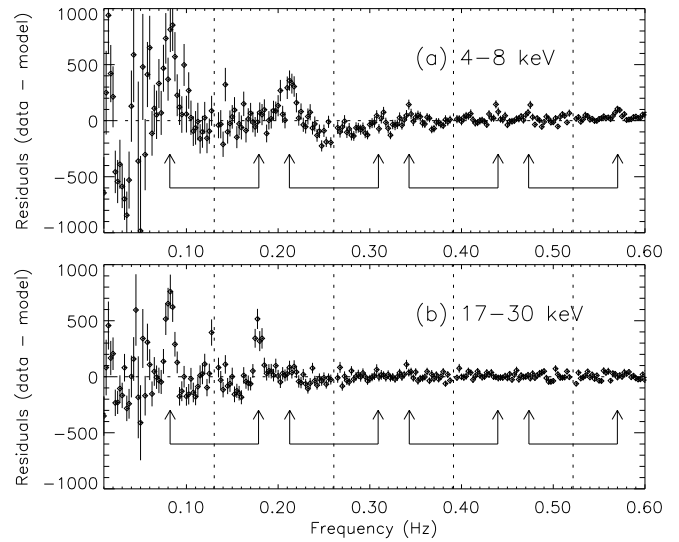


Fig. 2.— Residuals produced by subtracting the best-fit models from the pulse-subtracted power spectra. Vertical dotted lines show the positions where the sharp peaks due to the coherent pulsations have been removed. Pairs of arrows show the positions expected for symmetric sidebands if the QPO signal modulates the amplitude of the coherent pulsations.

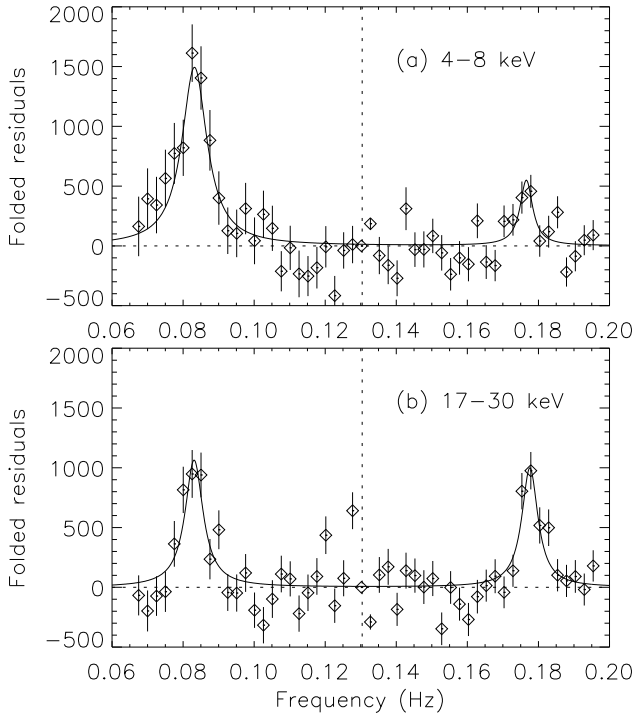


Fig. 3.— Folded residuals (see text). Vertical dotted lines show the position where the harmonic peaks have been shifted to 130 mHz. The solid line shows the best-fit Lorentzian functions to these residuals.